Hybrid Quantum System with Nitrogen-Vacancy Centers in Diamond Coupled to Surface-Phonon Polaritons in Piezomagnetic Superlattices

Peng-Bo Li (李蓬勃)[1,2,*] and Franco Nori (野理)[2,3]

[1]*Shaanxi Province Key Laboratory of Quantum Information and Quantum Optoelectronic Devices, Department of Applied Physics, Xi'an Jiaotong University, Xi'an 710049, China*

[2]*Theoretical Quantum Physics Laboratory, RIKEN Cluster for Pioneering Research, Wako-shi, Saitama 351-0198, Japan*

[3]*Department of Physics, The University of Michigan, Ann Arbor, Michigan 48109-1040, USA*

(Received 3 January 2018; revised manuscript received 18 June 2018; published 10 August 2018)

We investigate a hybrid quantum system where an ensemble of nitrogen-vacancy (NV) centers in diamond is interfaced with a piezomagnetic superlattice that supports surface-phonon polaritons (SPHPs). We show that the strong magnetic coupling between the collective spin waves in the NV spin ensemble and the quantized SPHPs can be realized, due to the subwavelength nature of the SPHPs and relatively long spin-coherence times. The magnon-polariton coupling allows different modes of the SPHPs to be mapped and orthogonally stored in different spatial modes of excitation in the solid medium. Because of its easy implementation and high tunability, the proposed hybrid structure with NV spins and piezoactive superlattices could be used for quantum memory and quantum computation.

DOI: 10.1103/PhysRevApplied.10.024011

I. INTRODUCTION

Electron spins in solids are promising candidates for quantum memory and quantum computation because of their long coherence time and perfect compatibility with other solid-state setups [1–9]. In hybrid quantum systems, coherent coupling between ensembles of nitrogen-vacancy (NV) centers in diamond and superconducting quantum circuits has been demonstrated [10–14]. To further explore the potential of spin ensembles, spatial modes of collective spin excitations can be used to encode a register of qubits [15–17], which allows the implementation of holographic quantum computing [18]. However, for superconducting quantum circuits, due to the long wavelength nature of microwave fields, they can only directly couple to collective spin excitations with a vanishing phase variation. This directly limits the ability to process quantum information in a spin ensemble via microwave photons. To make the best use of holographic techniques in spin ensembles, it is very appealing to coherently couple single microwave photons with collective spin-wave excitations. This is quite challenging in current experiments involving superconducting cavities, since the free wavelength of microwave photons is always much larger than the dimensions of spin ensembles. Here, we propose a protocol for this problem by coupling an ensemble of NV spins in diamond to surface-phonon polaritons (SPHPs) in piezomagnetic superlattices.

SPHPs are electromagnetic surface modes resulting from the coupling between crystal vibrations and electromagnetic fields [19–23]. Analogous to surface-plasmon polaritons [24–35], SPHPs tightly bound to the surface of a dielectric material often have a subwavelength confinement [36–38]. A piezoactive superlattice is a type of ordered microstructure, where the piezoelectric or piezomagnetic coefficient is periodically modulated [39–43]. SPHPs in piezoactive superlattices can be tailored with engineered frequencies and bandwidths via a suitable design of the superlattice [43,44]. This opens the possibility for generating SPHPs of microwave frequencies that can interact with ensembles of NV spins.

We show that there indeed exist SPHPs confined near the surface of a piezomagnetic superlattice formed by alternating layers of piezomagnetic materials. Then we provide a full quantum theory to describe the magnetic coupling between the collective spin-wave excitations of the NV spin ensemble and the quantized SPHP modes in the piezomagnetic superlattice. When taking into account the dissipations of SPHPs and NV centers, coherent couplings can dominate the interactions and the strong coupling regime can be realized. The achieved coupling strength can be the same order of magnitude as that associated with superconducting quantum circuits [10–14]. Unlike earlier work employing superconducting qubits or resonators, this hybrid structure exploits the magnon-SPHP coupling, and takes advantage of the subwavelength nature of SPHPs and the excellent tunability and scalability of piezoactive superlattices [39–43]. This

*lipengbo@mail.xjtu.edu.cn

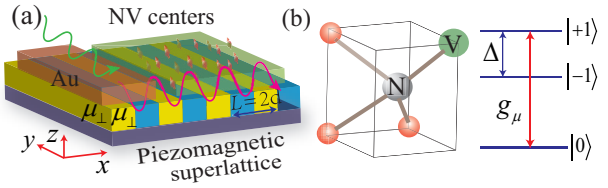

FIG. 1. (a) Schematic of an ensemble of NV centers in a diamond crystal located on the surface of a piezomagnetic superlattice with a period $L = 2d$, and dimensions $50 \times 2 \times 0.5$ mm^3. The surface lies in the x-y plane, while the SPHPs propagate along the x direction, where x, y, and z are the principle axes of the piezomagnetic crystal. Because a uniaxial material is used, we assume that the z axis is the optical axis, which defines $\mu^{(x)} = \mu^{(y)} = \mu_\perp$, and $\mu^{(z)} = \mu_\parallel$. (b) Schematic of a NV center with its vacancy (V) and nitrogen atom (N), as well as three neighboring carbon atoms (left); energy level diagram of the NV center (right).

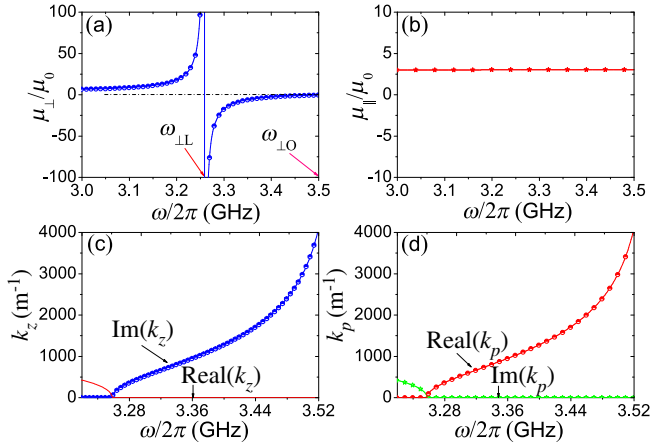

FIG. 2. (a),(b) Calculated effective permeability in the piezomagnetic superlattice formed by Terfenol-D with a period of 1 μm. (c),(d) Dispersion relation of SPHPs on a plane interface between vacuum and the piezomagnetic superlattice.

strong, and tunable magnon-polariton coupling allows the implementation of holographic techniques with this hybrid structure [15–17]. The combined NV spin and piezomagnetic superlattice approach opens routes for constructing hybrid quantum devices [45–54] with solid-state artificial structures, and could have wide applications in a range of fields: from nanophotonics [55–59] to quantum-information processing [60–63].

II. SETUP

As sketched in Fig. 1(a), an ensemble of NV centers in a diamond crystal is positioned above the surface of a semi-infinite periodic structure composed of alternating layers of piezomagnetic materials such as Terfenol-D or $CoFe_2O_4$. This kind of periodic artificial structure, with the piezomagnetic coefficient being periodically modulated, forms the so-called piezomagnetic superlattice [42]. In this setup, a negative permeability can be realized, and a type of phonon polariton typically bound to the interface between the surrounding medium and the piezomagnetic material can be created [64]. A semi-infinite gold (Au) film is deposited on top of the superlattice, which is used as a broadband antenna for converting the incident microwave field into strongly confined near fields at the gold edge [36,65].

We consider a piezomagnetic superlattice formed by Terfenol-D with a period of 1 μm. Figures 2(a) and 2(b) display the calculated effective permeability $\mu_\perp$ and $\mu_\parallel$, respectively, of the piezomagnetic superlattice [64]. As seen, for frequencies $\omega_{\perp L} < \omega < \omega_{\perp o}$, the effective permeability $\mu_\perp$ is negative, while $\mu_\parallel$ is positive. The permeability tensor is invariant with respect to rotations about the z axis. If we then consider the frequency of a surface polariton of propagation vector $\vec{k}_p$, the presence of the rotational symmetry of the permeability tensor means that the frequency must be independent of the orientation of the in-plane wavevector $\vec{k}_p$ relative to the x and y axes [20,23]. Therefore, the surface-polariton dispersion relation is independent of the direction of $\vec{k}_p$.

To derive the form of the dispersion relation, with no loss of generality, we may assume that the propagation vector $\vec{k}_p$ lies along the x direction [20,23]. Figures 2(c) and 2(d) show the dispersion relation for SPHPs propagating along the interface between vacuum and the piezomagnetic superlattice [64]. We find that, in the spectral gap, the in-plane wavevector is purely real, while the wave vector normal to the surface is purely imaginary [66,67]. Thus, the fields remain localized and only propagate along the interface. Based on the results in Fig. 2(d), we estimate that the wavelength for the SPHP of frequency $\omega \sim 2\pi \times 3.4$ GHz is about $\lambda_p \sim 6$ mm, which is about one order smaller than the free-space wavelength ($\lambda_0 \sim 9$ cm) or that of microwave photons in a superconducting cavity. In this case, the effective volume of the electromagnetic fields can be significantly reduced near the SPHP resonance, which leads to a strong field enhancement.

We assume the SPHPs propagate along the x direction with the surface normal along the z axis. The SPHPs can be approximated as TE fields with the magnetic field in the x-z plane. In this case, the quantized magnetic field of the SPHP with mode $\vec{k}$ becomes [64]

$$\vec{B}_{\vec{k}} = \sqrt{\frac{\hbar\omega(\vec{k})\mu_0}{2S}}\vec{b}_{\vec{k}}(z)\hat{a}_{\vec{k}}e^{ik_p x - i\omega(\vec{k})t} + \text{H.c.}, \qquad (1)$$

where $\omega(\vec{k})$ is the frequency, S is the quantization area, and $\hat{a}_{\vec{k}}$ is the destruction operator for mode $\vec{k}$. The polarization

vector $\vec{b}_{\vec{k}}(z)$ is given by [64]

$$\vec{b}_{\vec{k}}(z) = \mathcal{L}^{-1/2}(\vec{k}) e^{-\mathrm{Im}(k_z)z} \left(\vec{e}_x - \frac{k_p}{k_z} \vec{e}_z \right). \tag{2}$$

Here $\mathcal{L}(\vec{k})$ is the effective length of the mode, which depends on the geometry and magnetic response of the superlattice, and $\vec{e}_x$ and $\vec{e}_z$ are the unit vectors in the x and z directions.

III. COUPLING SPHP MODES TO SPIN WAVES

We now proceed to consider the coupling between NV spins and SPHPs. NV centers in diamond consist of a substitutional nitrogen atom and an adjacent vacancy, which have a spin $S = 1$ ground state, with zero-field splitting $D = 2\pi \times 2.87$ GHz, between the $|m_s = \pm 1\rangle$ and $|m_s = 0\rangle$ states. For moderate applied magnetic fields (B_z about several millitesla, and compatible with the SPHP modes), which cause Zeeman shifts of the states $|m_s = \pm 1\rangle$, one of the spin transitions of the NV center can be tuned into resonance with the SPHP mode. This allows us to isolate a two-level subsystem comprising $|m_s = 0\rangle$ and $|m_s = +1\rangle$, as shown in Fig. 1(b).

The interaction of a single NV center located at $\vec{r}_0$ with the total magnetic field can be written as

$$\hat{H}_{\mathrm{NV}} = \hbar D \hat{S}_z^2 + \mu_B g_s B_z \hat{S}_z + \mu_B g_s \vec{B}_{\vec{k}}(\vec{r}_0) \cdot \hat{\vec{S}}, \tag{3}$$

with $g_s = 2$ the Landé factor of the NV center, μ_B the Bohr magneton, and $\hat{\vec{S}}$ the spin operator of the NV center. Under the condition $|\Delta/2 + D - \omega(\vec{k})| \ll \Delta/2$, with $\Delta = 2\mu_B g_s B_z/\hbar$, we can neglect the state $|m_s = -1\rangle$, due to the external field moving it far out of resonance. Then we can derive the following Hamiltonian that describes the interaction between a single NV spin and a SPHP mode $\vec{k}$ [64]:

$$\hat{\mathcal{H}}_{\vec{k}} = \frac{1}{2}\hbar\omega_0 \hat{\sigma}_z + \hbar\omega(\vec{k}) \hat{a}_{\vec{k}}^\dagger \hat{a}_{\vec{k}} + \frac{\hbar g_\mu(\vec{k}, z_0)}{\sqrt{S}} \hat{\sigma}_+ \hat{a}_{\vec{k}} e^{ik_p x_0} + \mathrm{H.c.}, \tag{4}$$

with $\hat{\sigma}_z = |+1\rangle\langle+1| - |0\rangle\langle 0|$, $\hat{\sigma}_+ = |+1\rangle\langle 0|$, $\hbar\omega_0 = \hbar D + \mu_B g_s B_z$, and

$$g_\mu(\vec{k}, z_0) = \frac{\mu_B g_s}{2} \sqrt{\frac{\omega(\vec{k})\mu_0}{\hbar \mathcal{L}(\vec{k})}} e^{-\mathrm{Im}(k_z)z_0}. \tag{5}$$

We now consider the coupling between the NV spin ensemble and the SPHP modes. As depicted in Fig. 1(a), an ensemble of NV centers is doped into a diamond crystal of thickness h, and located at positions $\vec{r}_i$, each of which with a fixed quantization axis pointing along one of the four possible crystallographic directions. If the orientations are equally distributed among the four possibilities, and the external field is homogeneous, then a quarter of the NV spins can be made resonant with the SPHP mode. In such a case, we have the following Hamiltonian for N NV spins in the resonant subensemble interacting with the quantized surface mode $\vec{k}$:

$$\hat{\mathcal{H}}_{\vec{k}}^N = \sum_{i=1}^N \frac{1}{2}\hbar\omega_i \hat{\sigma}_z^i + \hbar\omega(\vec{k}) \hat{a}_{\vec{k}}^\dagger \hat{a}_{\vec{k}} + \sum_{i=1}^N \frac{\hbar g_\mu(\vec{k}, z_i)}{\sqrt{S}} (\hat{\sigma}_+^i \hat{a}_{\vec{k}} e^{ik_p x_i} + \mathrm{H.c.}), \tag{6}$$

where $\omega_i = \omega_0 + \delta_i$, and δ_i are random offsets accounting for the inhomogeneous broadening of the spin ensemble. These inhomogeneous broadening terms are usually on the order of megahertzs, whose effect can be described by spin dephasing.

To further simplify the model, we introduce the collective operators for the spin-wave modes in the NV ensemble

$$\hat{S}_{\vec{k}}^\dagger = \frac{1}{\sqrt{N} g_\mu^N(\vec{k})} \sum_{i=1}^N g_\mu(\vec{k}, z_i) \hat{\sigma}_+^i e^{ik_p x_i}, \tag{7}$$

with $g_\mu^N(\vec{k}) = \sqrt{\sum_{i=1}^N |g_\mu(\vec{k}, z_i)|^2/N}$. These spin-wave modes are orthogonal if the size of the diamond is much larger than the wavelength of the SPHP modes, and the separation between the NV spins is smaller than the SPHP wavelength. We consider the commutator $[\hat{S}_{\vec{k}_i}, \hat{S}_{\vec{k}_j}^\dagger] \equiv D(\vec{k}_j - \vec{k}_i)$ in the fully polarized limit. We find that

$$D(\vec{k}_j - \vec{k}_i) \sim \frac{1}{N} \int_{-l/2}^{l/2} e^{-i(k_{p,i} - k_{p,j})x} dx, \tag{8}$$

with l the extent of the sample along the x direction. When $\Delta k = k_{p,i} - k_{p,j} = 2\pi/l$, the mode overlap $D(\vec{k}_j - \vec{k}_i) = 0$, which means the spin-wave modes in the strongly polarized limit are orthogonal.

Then we have the following effective interaction Hamiltonian between the SPHP mode $\hat{a}_{\vec{k}}$ and the spin wave $\hat{S}_{\vec{k}}$:

$$\hat{\mathcal{H}}_{\vec{k}}^I = \hbar G_\mu^N(\vec{k}) (\hat{S}_{\vec{k}}^\dagger \hat{a}_{\vec{k}} + \mathrm{H.c.}). \tag{9}$$

Here the collective coupling strength is given by

$$G_\mu^N(\vec{k}) = g_\mu^N(\vec{k}) \sqrt{\frac{N}{S}} = \sqrt{\frac{1}{S} \sum_{i=1}^N |g_\mu(\vec{k}, z_i)|^2} = \frac{1}{2} \sqrt{n \int_0^h |g_\mu(\vec{k}, z)|^2 dz}, \tag{10}$$

where we assume a continuum of layers in the z direction with a thickness h, and a volume density of NV spins $n = 4N/(Sh)$. Obviously, the effective coupling strength between the NV spins and the quantized surface field is enhanced by a factor of $\sqrt{n}$. According to Eq. (9), the SPHP mode and the spin-wave mode behave as two coupled oscillators with a coupling strength $G_\mu^N(\vec{k})$. This allows any states of the two systems to be interchangeably mapped between them.

It is very useful to compare the coupling between NV spins and SPHPs with that between spin ensembles and other setups [10–12,14]. In this hybrid system, the surface-polariton modes are coupled to collective electron-spin-wave excitations in the spin ensemble, in direct contrast with other setups involving superconducting qubits or resonators [10–12,14]. For the latter, only the collective spin excitations with a vanishing phase variation are employed, because of the long wavelength nature of microwave fields. However, in our proposed device, even though it works in the microwave range, the spatial modes of spin excitations must be considered, due to the subwavelength nature of the SPHPs. This will be very useful for holographic quantum computation with spin ensembles, which employs collective spin-wave excitations to encode a register of qubits [15–18].

In Fig. 3, we plot the calculated single-spin coupling constant $g_\mu(\vec{k},z)$ and the collective coupling $G_\mu^N(\vec{k})$ as a function of the frequency within the negative gap. From Fig. 3(a), we find that obviously g_μ varies with the distance z and decreases as z increases, which indicates that the SPHP modes decay exponentially along the direction normal to the interface. Figure 3(b) shows that the collective coupling strength $G_\mu^N(\vec{k})$ depends strongly on the thickness h but tends to saturate for thick enough crystals. When $\omega \sim 2\pi \times 3.4$ GHz, the collective coupling strength can reach $2\pi \times 9$ MHz. This coupling strength is comparable

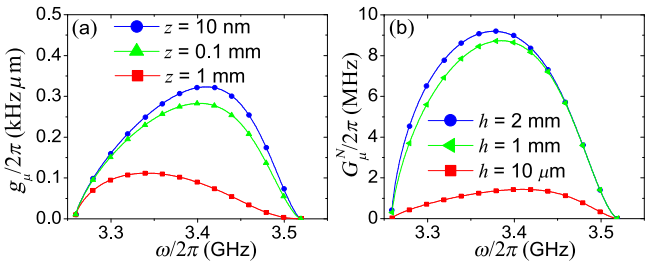

FIG. 3. (a) Coupling constant $g_\mu(\vec{k},z)$ of a single NV spin for different positions z interacting with a SPHP mode with the wavevector $\vec{k}$. (b) Collective coupling constant $G_\mu^N(\vec{k})$ of a NV center ensemble in a diamond crystal with dimensions $20 \times 2 \times h$ mm^3 and a density of $n \sim 2 \times 10^6$ μm^{-3} (about 6 ppm) [10,12] for different values of thickness h. Other parameters are chosen as those in Fig. 2.

to that of a NV spin ensemble coupled to a superconducting flux qubit [11,14] or a coplanar waveguide cavity [10,12].

In actual crystals, due to scattering, absorption, and other process, the decay of the SPHP mode ($\kappa_{\rm SPHP}$) should be taken into consideration [64]. It has been shown [20] that the decay of the SPHP mode is frequency dependent, and near the SPHP resonance frequency, the SPHP decay is approximately equal to the damping constant of the crystal. For piezomagnetic crystals like Terfenol-D or $CoFe_2O_4$, the damping constant can be approximated as $\Gamma \sim 0.001\omega_0$ [41], with ω_0 the resonance frequency for the SPHP mode. In this case, we can estimate the decay of the SPHP mode as $\kappa_{\rm SPHP} \sim 2\pi \times 3.4$ MHz. To further increase the Q factor of the surface modes so that the strong-coupling regime can be entered more easily, two main strategies can be pursued. The first concentrates on reducing the damping of the material. The second exploits cavities incorporated into superlattice structures [57,58,61], which can combine the benefits of a high Q factor and small mode volume.

For NV spins, the T_2 time for a spin ensemble may be reduced to T_2^* because of interactions with nearby lattice nuclei and paramagnetic impurities [64]. The hyperfine interaction with lattice ^{13}C will be detrimental to the electron spin coherence, but this can be overcome when using isotopically purified ^{12}C diamond. For ^{14}N nuclear spin, due to its long relaxation time, the nuclear spin does not lead to decoherence but can actually be used as a resource for quantum memory. Recent experiments demonstrate that the dephasing time for a NV spin ensemble is still in the microsecond range, with $\gamma_s \sim 2\pi \times 3$ MHz [10]. If other methods, such as the spin-echo techniques, are used [68], then the spin-dephasing time will be extended from T_2^* to T_2, which is close to the intrinsic spin-coherence time (on the order of kilohertz).

A useful measure of the coupling efficiency is the cooperativity $C = (G_\mu^N)^2/(\gamma_s\kappa_{\rm SPHP})$. The strong coupling regime can be reached if the collective coupling strength $G_\mu^N(\vec{k})$ exceeds both the electronic spin-dephasing rate γ_s and the intrinsic damping rate of the SPHP mode $\kappa_{\rm SPHP}$, $G_\mu^N(\vec{k}) > \{\gamma_s, \kappa_{\rm SPHP}\}$, i.e., $C > 1$. Figure 4(a) shows the cooperativity decreasing as the superlattice period $L = 2d$ increases. In our hybrid magnon-polariton system, we choose $L = 2d = 1$ μm, and obtain $C \sim 90$ with a moderate spin-dephasing rate. Moreover, in Fig. 4(b), we plot the eigenfrequencies $\omega_\pm$ of the coupled magnon-polariton system as the spin-transition frequency is varied through resonance with the SPHP mode by changing the Zeeman splitting. The avoided crossing with a clear splitting shows that the magnon mode strongly couples to the SPHP mode.

We now consider the preparation and detection of the relevant states of the hybrid system. NV centers can be prepared in their ground spin state $|m_s = 0\rangle$ by using

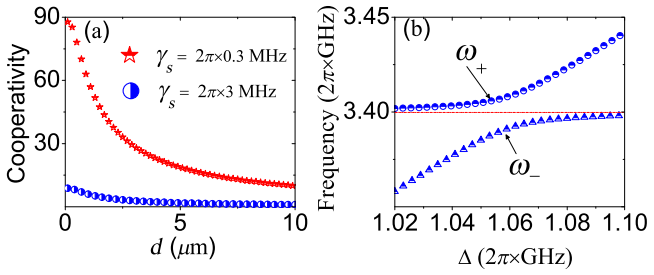

FIG. 4. (a) Cooperativity C as a function of the superlattice period $L = 2d$. Here $\kappa_{\mathrm{SPHP}} \sim 0.001\omega_{\perp L}$, and $h = 1$ mm. Other parameters are chosen the same as those in Fig. 3. (b) Eigenfrequencies of the coupled magnon-polariton system. Here $G_\mu^N = 2\pi \times 9$ MHz, $\gamma_s \sim 0.2\, G_\mu^N$, and $\kappa_{\mathrm{SPHP}} \sim 0.3\, G_\mu^N$.

the spin-selective optical-pumping method [17]. As for SPHPs, it is possible to excite a SPHP mode with a fixed wave vector by applying the edge-launching or edge-coupling method [36,69]. Actually, a recent experiment [65], has demonstrated that SPHPs with the plane-wave propagation can be launched at the edge of a semi-infinite gold film deposited on top of a hexagonal boron nitride slab. Therefore, we may envision that, in principle, the same approach can be used in our setup to excite a plane-wave SPHP mode in a piezomagnetic superlattice. In this way, the SPHP mode with the propagating wave vector $\vec{k}_p$ can produce a continuous-wave magnetic field near the surface, which will strongly couple to the collective spin-wave mode described by $\hat{S}_{\vec{k}}$. Then, the state of a SPHP mode will be mapped to a specific spin wave. Excitations stored in this way may be detected by applying a gradient pulse that converts a particular spin wave back into a uniform transverse magnetization [15–17]. As demonstrated in recent experiments [9,70], a direct measurement of the spin polarization can be realized by optically detected magnetic resonance.

IV. STORAGE OF DIFFERENT SPHP MODES

Since the k modes of the spin ensemble in the strongly polarized limit behave as a large number of independent harmonic oscillators, it is possible to orthogonally store multiple SPHP modes in these spin-wave modes with the magnon-polariton coupling. We consider the storage of two different SPHP modes with the propagation vectors k_1 and k_2, and the polariton operators $\hat{a}_{\vec{k}_1}$ and $\hat{a}_{\vec{k}_2}$. As described above, the propagation vectors should satisfy $|k_1 - k_2| = 2\pi/l \sim 314$ to ensure that the corresponding spin-wave modes are orthogonal. Based on the results given in Figs. 2(b) and 3(b), we find that these modes exist and can strongly couple to the spin waves. So if the SPHP modes k_1 and k_2 are excited by, for instance, the edge-launching method, then with the interaction described by Eq. (9), we can map the states of the SPHP modes into the collective spin-wave modes $\hat{S}_{\vec{k}_1}$ and $\hat{S}_{\vec{k}_2}$, through the swap gate $\hat{U}_{\mathrm{sw}} = e^{-i\hat{\mathcal{H}}_{\vec{k}}^I T_{\pi/2}/\hbar}$, with $T_{\pi/2} = \pi/(2G_\mu^N)$. In principle, the above procedure can apply to the general multimode storage case.

V. CONCLUSIONS

We propose a hybrid quantum device where an ensemble of NV centers in a diamond crystal is interfaced with a piezomagnetic superlattice supporting SPHPs. We show that the magnetic coupling between the collective spin waves and SPHPs can be tailored through a suitable design of the piezomagnetic superlattice. This strong magnon-polariton coupling allows us to implement the holographic techniques with this hybrid device. Such a device could also be used as a coherent interface for other quantum systems such as superconducting qubits, cold atoms, and polar molecules.

ACKNOWLEDGEMENT

P.B.L. acknowledges helpful discussions with Peter Rabl, Carlos Sánchez Muñoz, Zhou Li, and Jiteng Sheng. P.B.L was supported by the NSFC under Grants No. 11774285 and 11474227. F.N. was supported in part by the MURI Center for Dynamic Magneto-Optics via the Air Force Office of Scientific Research (AFOSR) (FA9550-14-1-0040), Army Research Office (ARO) (Grant No. 73315PH), Asian Office of Aerospace Research and Development (AOARD) (Grant No. FA2386-18-1-4045), Japan Science and Technology Agency (JST) (the ImPACT program and CREST Grant No. JPMJCR1676), Japan Society for the Promotion of Science (JSPS) (JSPS-RFBR Grant No. 17-52-50023), RIKEN-AIST Challenge Research Fund, and the John Templeton Foundation.

APPENDIX A: THEORY OF SURFACE-PHONON POLARITONS IN PIEZOMAGNETIC SUPERLATTICES

1. Phonon polaritons in a piezomagnetic superlattice

We study electromagnetic waves propagating in a semi-infinite periodic structure composed of alternating layers of piezomagnetic materials such as Terfenol-D or $CoFe_2O_4$. This kind of periodic artificial structure, with the piezomagnetic coefficient being periodically modulated, forms the so-called piezomagnetic superlattice [42]. In this artificial microstructure, the lattice vibrations will induce spin waves because of the piezomagnetic effect. Because the produced spin waves will in turn emit electromagnetic waves that interfere with the original electromagnetic waves, the lattice vibration will couple strongly with the electromagnetic waves, leading to polariton excitations. Near the piezomagnetic polariton resonance, an effective negative permeability can be implemented.

As displayed in Fig. 1, the piezomagnetic superlattice is arranged along the x axis, and we assume the transverse dimensions are very large compared with an acoustic wavelength so that a one-dimensional model is valid. The piezomagnetic equations describing the interaction between electromagnetic waves and acoustic waves are [42,71,72]

$$T_{ij} = c_{ijkl}u_{kl} + q_{ijk}H_k, \tag{A1}$$

$$B_i = \mu^s_{ik}H_k - q_{ikl}u_{kl}, \tag{A2}$$

where T_{ij}, B_i, H_k are the stress tensor, magnetic displacement, and magnetic field; $c_{ijkl}, u_{kl}, q_{ijk}$ are the elastic tensor, strain tensor, and piezomagnetic coefficient; μ^s_{ik} is the static magnetic permeability. The piezomagnetic coefficient is periodically modulated with the form

$$q(x) = \begin{cases} +q & \text{in positive domains} \quad (0 \le x < d), \\ -q & \text{in negative domains} \quad (d \le x < 2d). \end{cases} \tag{A3}$$

From Newton's law $\rho\partial^2 u_j/\partial t^2 = (\partial/\partial x_i)T_{ij}$, we have

$$\rho\frac{\partial^2 u_j}{\partial t^2} = c_{ijkl}\frac{\partial^2 u_k}{\partial x_i \partial x_l} + \frac{\partial[q_{ijk}(x)H_k]}{\partial x_i}, \tag{A4}$$

with u_j being the displacement along the Cartesian coordinate x_j $(x_1 = x, x_2 = y, x_3 = z)$, and ρ the mass density. If the x_1-x_2 plane is taken as the isotropic plane of materials, the piezomagnetic tensor matrix can be written in the Voigt form [42,71,72]

$$q = \begin{pmatrix} 0 & 0 & 0 & 0 & q_{15} & 0 \\ 0 & 0 & 0 & q_{15} & 0 & 0 \\ q_{31} & q_{31} & q_{33} & 0 & 0 & 0 \end{pmatrix} \tag{A5}$$

and the elastic coefficient has the form [42,71,72]

$$C = \begin{pmatrix} c_{11} & c_{12} & c_{13} & 0 & 0 & 0 \\ c_{12} & c_{11} & c_{13} & 0 & 0 & 0 \\ c_{13} & c_{13} & c_{33} & 0 & 0 & 0 \\ 0 & 0 & 0 & c_{44} & 0 & 0 \\ 0 & 0 & 0 & 0 & c_{44} & 0 \\ 0 & 0 & 0 & 0 & 0 & c_{66} \end{pmatrix}. \tag{A6}$$

The static magnetic permeability tensor is

$$\mu = \begin{pmatrix} \mu^s_{11} & 0 & 0 \\ 0 & \mu^s_{11} & 0 \\ 0 & 0 & \mu^s_{33} \end{pmatrix}. \tag{A7}$$

With the above equations we can solve the piezomagnetic problem by using the Fourier transformation. First, we solve a simple one-dimensional model, which can be generalized to a more general case. The piezomagnetic equations pertaining to this case are

$$T_{11} = c_{11}u_{11} + q_{31}H_3 = c_{11}\frac{\partial u_1}{\partial x} + q_{31}(x)H_3, \tag{A8}$$

$$B_3 = \mu^s_{11}H_3 - q_{31}(x)u_{11}, \tag{A9}$$

$$\rho\frac{\partial^2 u_1}{\partial t^2} = c_{11}\frac{\partial^2 u_1}{\partial x^2} + \frac{\partial[q_{31}(x)H_3]}{\partial x}. \tag{A10}$$

By using the Fourier transformation

$$\begin{aligned} u_1(x,t) &= \int u(q)e^{i(\omega t - qx)}dq, \\ H_3(x,t) &= \int H(k)e^{i(\omega t - kx)}dk, \\ q_{31}(x) &= \sum_{m\neq 0}\frac{i(1-\cos m\pi)}{m\pi}q_{31}e^{-iG_m x} \\ &= \sum_{m\neq 0}F_m q_{31}e^{-iG_m x} \quad \text{where } G_m = m\frac{\pi}{d}, \end{aligned} \tag{A11}$$

we have

$$\begin{aligned} &\int(\rho\omega^2 - c_{11}q^2)u(q)e^{-qx}dq \\ &= -\frac{\partial}{\partial x}\left[\sum_m F_m q_{31}e^{-iG_m x}\int H(k)e^{-ikx}dk\right] \\ &= -\int\sum_m F_m q_{31}(-i)(k+G_m)H(k)e^{-i(k+G_m)x}dk. \end{aligned} \tag{A12}$$

For photons with long wavelength $k \to 0$ or $k \ll G_m$, Eq. (A12) becomes

$$\begin{aligned} &\int(\rho\omega^2 - c_{11}q^2)u(q)e^{-qx}dq \\ &= \sum_m iF_m q_{31}G_m H(k)e^{-i(k+G_m)x}. \end{aligned} \tag{A13}$$

In order to make the two sides equal, $q = k + G_m$ must be satisfied. Then we have

$$u_1(q = k + G_m) = iF_m q_{31}\frac{G_m}{\rho\omega^2 - c_{11}G_m^2}H(k) \tag{A14}$$

and

$$u_{11}(x,t) = \int \left[F_m q_{31} \frac{G_m^2}{\rho\omega^2 - c_{11}G_m^2} H(k) e^{i(\omega t - kx)} e^{-iG_m x} \right] dk$$
$$= F_m q_{31} \frac{G_m^2}{\rho\omega^2 - c_{11}G_m^2} e^{-iG_m x} H_3(x,t)$$
$$= \varphi(x) H_3(x,t). \tag{A15}$$

Substituting Eq. (A15) into Eq. (A10), we have

$$B_3 = \mu_{11}^s H_3 - q_{31}(x)\varphi(x) H_3(x,t)$$
$$= \mu(x)\mu_0 H_3(x,t). \tag{A16}$$

For long wavelength $k \to 0$, the piezomagnetic superlattice can be assumed to be homogeneous, and the space average value of $\mu(x)$ should be used [40]:

$$\tilde{\mu}_\perp(\omega) = \mu_\perp(\omega)\mu_0$$
$$= \mu_{11}^s + \frac{1}{2d}\int_0^{2d} \mu(x)dx$$
$$= \mu_{11}^s + \frac{q_{31}^2/d^2\rho}{\omega_{\perp L}^2 - \omega^2}$$
$$= \mu_{11}^s \frac{\omega_{\perp o}^2 - \omega^2}{\omega_{\perp L}^2 - \omega^2}, \tag{A17}$$

with

$$\omega_{\perp L}^2 = c_{11}\pi^2/\rho d^2, \tag{A18}$$

$$\omega_{\perp o}^2 = \omega_{\perp L}^2 + q_{31}^2/d^2\rho\mu_{11}^s. \tag{A19}$$

Based on the same reasoning [42], we obtain the following relations:

$$\mu_\parallel(\omega) = \mu_{33}^s/\mu_0 \frac{\omega_{\parallel o}^2 - \omega^2}{\omega_{\parallel L}^2 - \omega^2}, \tag{A20}$$

$$\omega_{\parallel L}^2 = c_{33}\pi^2/\rho d^2, \tag{A21}$$

$$\omega_{\parallel o}^2 = \omega_{\parallel L}^2 + q_{33}^2/d^2\rho\mu_{33}^s. \tag{A22}$$

Therefore, the effective magnetic permeability tensor is

$$\mu(\omega) = \begin{pmatrix} \mu_\perp(\omega) & 0 & 0 \\ 0 & \mu_\perp(\omega) & 0 \\ 0 & 0 & \mu_\parallel(\omega) \end{pmatrix}. \tag{A23}$$

2. The surface-phonon-polariton dispersion relation

We now discuss the electromagnetic waves propagating at the boundary between vacuum ($\epsilon_1 = 1, \mu_1 = 1$) and the piezomagnetic superlattice ($\epsilon_2, \mu_\perp, \mu_\parallel$). The permeability tensor is invariant with respect to rotations about the z axis. If we consider the frequency of a surface polariton of propagation vector $\vec{k}_p$, the presence of the rotational symmetry of the permeability tensor means that the frequency must be independent of the orientation of the in-plane wavevector $\vec{k}_p$ relative to the x and y axes [20,23]. Therefore, the surface-polariton dispersion relation is independent of the direction of $\vec{k}_p$. We consider the interface described in Fig. 1, where the surface lies in the x-y plane. To derive the form of the dispersion relation, with no loss of generality, we may assume that the propagation vector $\vec{k}_p$ lies along the x direction [20,23], and look for TE wave solutions of Maxwell's equations in which the magnetic fields vary as the following form in both media [23]:

$$\vec{H}_1 = \begin{pmatrix} H_{1x} \\ 0 \\ H_{1z} \end{pmatrix} e^{ik_{p1}x - i\omega t} e^{ik_{1z}z}, \tag{A24}$$

$$\vec{H}_2 = \begin{pmatrix} H_{2x} \\ 0 \\ H_{2z} \end{pmatrix} e^{ik_{p2}x - i\omega t} e^{ik_{2z}z} \tag{A25}$$

and the electric fields are in the y direction:

$$\vec{E}_1 = \begin{pmatrix} 0 \\ E_{1y} \\ 0 \end{pmatrix} e^{ik_{p1}x - i\omega t} e^{ik_{1z}z}, \tag{A26}$$

$$\vec{E}_2 = \begin{pmatrix} 0 \\ E_{2y} \\ 0 \end{pmatrix} e^{ik_{p2}x - i\omega t} e^{ik_{2z}z}. \tag{A27}$$

The $\vec{k}$ vector parallel to the interface is conserved,

$$k_{p1} = k_{p2} = k_p. \tag{A28}$$

From the boundary condition $\vec{n} \times (\vec{H}_2 - \vec{H}_1) = 0$, we have

$$H_{1x} = H_{2x} = H_x. \tag{A29}$$

The wave numbers in medium 1 satisfy

$$k_p^2 + k_{1z}^2 = \epsilon_1\mu_1 k_0^2 = \frac{\omega^2}{c^2}. \tag{A30}$$

From $\nabla \cdot \vec{B} = 0$, we have

$$k_p H_x + k_{1z} H_{1z} = 0. \tag{A31}$$

In the magnetic superlattice, we have the following relations [23]:

$$\frac{k_p^2}{\mu_\parallel} + \frac{k_{2z}^2}{\mu_\perp} = k_0^2\epsilon_2, \tag{A32}$$

$$k_p\mu_\perp H_x + k_{2z}\mu_\parallel H_{2z} = 0. \tag{A33}$$

With Eqs. (A28) to (A33), we can obtain the following relations for the wave numbers [20,73]:

$$k_p^2 = \frac{(\mu_1\epsilon_2 - \mu_\perp)\mu_\parallel\mu_1}{\mu_1^2 - \mu_\perp\mu_\parallel}k_0^2, \tag{A34}$$

$$k_{1z}^2 = \frac{\mu_1 - \mu_\parallel\epsilon_2}{\mu_1^2 - \mu_\perp\mu_\parallel}k_0^2\mu_1^2, \tag{A35}$$

$$k_{2z}^2 = \frac{\mu_1 - \mu_\parallel\epsilon_2}{\mu_1^2 - \mu_\perp\mu_\parallel}k_0^2\mu_\perp^2. \tag{A36}$$

Based on Eqs. (A34)–(A36), and using the material parameters given in Table I [74,75], we can investigate the dispersion relation of SPHPs in the piezomagnetic superlattice. We find that there indeed exist SPHPs that propagate along the interface between vacuum and the piezomagnetic superlattice over a range of frequencies, within which the permeability $\mu_\perp$ along the propagation direction is negative, and $\mu_\parallel$ is positive, leading to the formation of a piezomagnetic superlattice. The numerical results are given in Fig. 2 in the main text. Through Eqs. (A28)–(A36), we can also obtain the relation between the field components:

$$\frac{|H_x|^2}{|H_{1z}|} = -\frac{k_{1z}^2}{k_p^2} = -\frac{\mu_1(\mu_1 - \mu_\parallel\epsilon_2)}{\mu_\parallel(\mu_1\epsilon_2 - \mu_\perp)}, \tag{A37}$$

$$\frac{|H_x|^2}{|H_{2z}|} = -\frac{\mu_\parallel^2 k_{2z}^2}{\mu_\perp^2 k_p^2} = -\frac{\mu_\parallel(\mu_1 - \mu_\parallel\epsilon_2)}{\mu_1(\mu_1\epsilon_2 - \mu_\perp)}. \tag{A38}$$

If we define

$$|H_x|^2 + |H_{1z}|^2 = |H_1|^2, \tag{A39}$$

$$|H_x|^2 + |H_{2z}|^2 = |H_2|^2, \tag{A40}$$

then we can obtain

$$\begin{aligned}|H_x|^2 &= -\frac{|H_1|^2\mu_1(\mu_1 - \mu_\parallel\epsilon_2)}{2\mu_1\mu_\parallel\epsilon_2 - \mu_1^2 - \mu_\parallel\mu_\perp} \\ &= -\frac{|H_2|^2\mu_\parallel(\mu_1 - \mu_\parallel\epsilon_2)}{\mu_1(\mu_1\epsilon_2 - \mu_\perp) - \mu_\parallel(\mu_1 - \mu_\parallel\epsilon_2)},\end{aligned} \tag{A41}$$

TABLE I. Material parameters for Terfenol-D considered in this work (see [74,75]).

Term	Value	Units
Mass density ρ	9.23×10^3	kg/m^3
c_{11}	5.5×10^{10}	N/m^2
c_{33}	5.5×10^{10}	N/m^2
c_{44}	1.2×10^{10}	N/m^2
q_{13}	-200	N/Am
q_{33}	400	N/Am
μ_{11}^s	6.23×10^{-6}	N^2/A
μ_{33}^s	6.23×10^{-6}	N^2/A
ϵ_2	10^3	...

$$|H_{1z}|^2 = \frac{|H_1|^2\mu_\parallel(\mu_1\epsilon_2 - \mu_\perp)}{2\mu_1\mu_\parallel\epsilon_2 - \mu_1^2 - \mu_\parallel\mu_\perp}, \tag{A42}$$

$$|H_{2z}|^2 = \frac{|H_2|^2\mu_1(\mu_1\epsilon_2 - \mu_\perp)}{\mu_1(\mu_1\epsilon_2 - \mu_\perp) - \mu_\parallel(\mu_1 - \mu_\parallel\epsilon_2)}. \tag{A43}$$

To obtain the relation for the electric field components, we employ Maxwell's equation

$$\vec{E} = \frac{i}{\omega\epsilon}\nabla \times \vec{H} \tag{A44}$$

and derive the following relations:

$$E_{1y} = E_{2y} = \frac{\mu_0 c^2}{\omega}(k_{1z}H_x - k_p H_{1z}), \tag{A45}$$

$$\frac{|H_1|^2}{|H_2|^2} = \frac{\mu_\parallel(2\mu_1\mu_\parallel\epsilon_2 - \mu_\parallel\mu_\perp - \mu_1^2)}{\mu_1[\mu_1(\mu_1\epsilon_2 - \mu_\perp) - \mu_\parallel(\mu_1 - \mu_\parallel\epsilon_2)]}, \tag{A46}$$

$$\begin{aligned}|E|^2 = |E_{1y}|^2 = |E_{2y}|^2 = \mu_0^2 c^2|H_1|^2\mu_1 \\ \times \frac{\mu_1^2 - \mu_\perp\mu_\parallel}{2\mu_1\mu_\parallel\epsilon_2 - \mu_\perp\mu_\parallel - \mu_1^2}.\end{aligned} \tag{A47}$$

3. Energy density

The density of electromagnetic field energy in a dispersive medium is given by [76]

$$U = \frac{1}{2}\left[\epsilon_0\frac{\partial(\omega\epsilon)}{\partial\omega}E^2 + \mu_0\frac{\partial(\omega\mu)}{\partial\omega}H^2\right]. \tag{A48}$$

Then in the upper space $z > 0$, we have

$$\begin{aligned}U_1 &= \frac{1}{4}(\epsilon_0|E_1|^2 + \mu_0\mu_1|H_1|^2)e^{-2|k_{1z}|z} \\ &= \frac{1}{2}\mu_0|H_1|^2\frac{\mu_1\mu_\parallel(\mu_1\epsilon_2 - \mu_\perp)}{2\mu_1\mu_\parallel\epsilon_2 - \mu_\perp\mu_\parallel - \mu_1^2}e^{-2|k_{1z}|z}.\end{aligned} \tag{A49}$$

In the superlattice $z < 0$, the electromagnetic density is

$$\begin{aligned} U_2 &= \frac{1}{4}(\mu_0\mu_\perp|H_x|^2 + \mu_0\mu_\parallel|H_{2z}|^2 \\ &\quad + \mu_0\omega\frac{\partial\mu_\perp}{\partial\omega}|H_x|^2 + \mu_0\omega\frac{\partial\mu_\parallel}{\partial\omega}|H_{2z}|^2 + \epsilon_2\epsilon_0|E|^2)e^{2|k_{2z}|z} \\ &= \frac{1}{4}\mu_0|H_2|^2\left[\frac{2\mu_1\mu_\parallel(\mu_1\epsilon_2-\mu_\perp)}{\mu_1(\mu_1\epsilon_2-\mu_\perp)-\mu_\parallel(\mu_1-\mu_\parallel\epsilon_2)}\right. \\ &\quad -\frac{\omega\mu_\parallel(\mu_1-\mu_\parallel\epsilon_2)}{\mu_1(\mu_1\epsilon_2-\mu_\perp)-\mu_\parallel(\mu_1-\mu_\parallel\epsilon_2)}\frac{\partial\mu_\perp}{\partial\omega} \\ &\quad \left.+\frac{\omega\mu_1(\mu_1\epsilon_2-\mu_\perp)}{\mu_1(\mu_1\epsilon_2-\mu_\perp)-\mu_\parallel(\mu_1-\mu_\parallel\epsilon_2)}\frac{\partial\mu_\parallel}{\partial\omega}\right]e^{2|k_{2z}|z}. \end{aligned} \tag{A50}$$

The total energy density associated with the SPHPs is determined by integration over z [20],

$$\begin{aligned} \langle U_1\rangle + \langle U_2\rangle &= \int_0^\infty U_1 dz + \int_{-\infty}^0 U_2 dz \\ &= \frac{1}{8}\mu_0\frac{|H_2|^2}{|k_{2z}|}M(\mu_1,\mu_\perp,\mu_\parallel,\omega,\epsilon_2) \\ &= \frac{1}{8}\mu_0\frac{|H_1|^2}{|k_{1z}|}F(\mu_1,\mu_\perp,\mu_\parallel,\omega,\epsilon_2), \end{aligned} \tag{A51}$$

with

$$\begin{aligned} &M(\mu_1,\mu_\perp,\mu_\parallel,\omega,\epsilon_2) \\ &= \frac{2\mu_1^2\mu_\parallel(\mu_1\epsilon_2-\mu_\perp)-2\mu_\parallel^2\mu_\perp(\mu_1\epsilon_2-\mu_\perp)}{\mu_1[\mu_1(\mu_1\epsilon_2-\mu_\perp)-\mu_\parallel(\mu_1-\mu_\parallel\epsilon_2)]} \\ &\quad -\frac{\omega\mu_\parallel(\mu_1-\mu_\parallel\epsilon_2)}{\mu_1(\mu_1\epsilon_2-\mu_\perp)-\mu_\parallel(\mu_1-\mu_\parallel\epsilon_2)}\frac{\partial\mu_\perp}{\partial\omega} \\ &\quad +\frac{\omega\mu_1(\mu_1\epsilon_2-\mu_\perp)}{\mu_1(\mu_1\epsilon_2-\mu_\perp)-\mu_\parallel(\mu_1-\mu_\parallel\epsilon_2)}\frac{\partial\mu_\parallel}{\partial\omega}, \end{aligned} \tag{A52}$$

and

$$\begin{aligned} &F(\mu_1,\mu_\perp,\mu_\parallel,\omega,\epsilon_2) \\ &= \frac{2\mu_1\mu_\perp\mu_\parallel(\mu_1\epsilon_2-\mu_\perp)-2\mu_1^3(\mu_1\epsilon_2-\mu_\perp)}{\mu_\perp(2\mu_1\mu_\parallel\epsilon_2-\mu_\perp\mu_\parallel-\mu_1^2)} \\ &\quad +\frac{\omega\mu_1^2\mu_\parallel(\mu_1-\mu_\parallel\epsilon_2)}{\mu_\perp\mu_\parallel(2\mu_1\mu_\parallel\epsilon_2-\mu_\perp\mu_\parallel-\mu_1^2)}\frac{\partial\mu_\perp}{\partial\omega} \\ &\quad -\frac{\omega\mu_1^3(\mu_1\epsilon_2-\mu_\perp)}{\mu_\perp\mu_\parallel(2\mu_1\mu_\parallel\epsilon_2-\mu_\perp\mu_\parallel-\mu_1^2)}\frac{\partial\mu_\parallel}{\partial\omega}. \end{aligned} \tag{A53}$$

4. Quantization of the surface fields

So far we treat the electric and magnetic fields with respect to surface-phonon polariotons as classical variables. The magnetic field in medium 1 is given by

$$\vec{H}_1 = A_{1k}\vec{u}_{1k}e^{ik_px-i\omega t}e^{ik_{1z}z} + \text{c.c.} \tag{A54}$$

with

$$\vec{u}_{1k} = \frac{1}{\sqrt{\mathcal{L}}}\left(\vec{e}_x - \frac{k_p}{k_{1z}}\vec{e}_z\right). \tag{A55}$$

A_{1k} is the amplitude that is related to the destruction operator for photons [77], and $\mathcal{L}$ has the dimension of a length and will be fixed later to normalize the energy of each mode [77].

The total energy of the surface waves is

$$\begin{aligned} S(\langle U_1\rangle + \langle U_2\rangle) &= S\frac{1}{8}\mu_0\frac{|H_1|^2}{|k_{1z}|}F \\ &= S\frac{1}{8}\mu_0\frac{4|A_{1k}|^2}{|k_{1z}|}\frac{1}{\mathcal{L}}\left(1+\frac{|k_p|^2}{|k_{1z}|^2}\right)F \\ &= 2\mu_0 S|A_{1k}|^2 = \mu_0 S A_{1k}^* A_{1k} + \mu_0 S A_{1k}A_{1k}^*. \end{aligned} \tag{A56}$$

We use the degree of freedom to set $\mathcal{L}$ to simplify the above equation, i.e., we choose

$$\begin{aligned} \mathcal{L} &= \frac{1}{4}\frac{F}{|k_{1z}|}\left(1+\frac{|k_p|^2}{|k_{1z}|^2}\right) \\ &= \frac{\mu_1(\mu_\parallel\epsilon_2-\mu_1)+\mu_\parallel(\mu_1\epsilon_2-\mu_\perp)}{4|k_{1z}|\mu_1(\mu_\parallel\epsilon_2-\mu_1)}F. \end{aligned} \tag{A57}$$

Then we find that the expression for the surface-wave energy (A56) has the structure of the energy of a harmonic oscillator. By taking the equivalence

$$A_{1k} \to \sqrt{\frac{\hbar\omega(\vec{k})}{2\mu_0 S}}\hat{a}_{\vec{k}} \qquad A_{1k}^* \to \sqrt{\frac{\hbar\omega(\vec{k})}{2\mu_0 S}}\hat{a}_{\vec{k}}^\dagger, \tag{A58}$$

we can obtain the quantized Hamiltonian of the surface wave with mode vector $\vec{k}$,

$$\hat{H} = \frac{1}{2}\hbar\omega(\vec{k})\left(\hat{a}_{\vec{k}}^\dagger\hat{a}_{\vec{k}} + \hat{a}_{\vec{k}}\hat{a}_{\vec{k}}^\dagger\right). \tag{A59}$$

The surface-wave field is thus quantized by association of a quantum-mechanical harmonic oscillator to each mode $\vec{k}$. The operators $\hat{a}_{\vec{k}}$ and $\hat{a}_{\vec{k}}^\dagger$ are annihilation and creation operators which destroy and create a quantum of SPHPs with energy $\hbar\omega(\vec{k})$, and obey bosonic commutation relations $[\hat{a}_{\vec{k}}, \hat{a}_{\vec{k}'}^\dagger] = \delta_{\vec{k}\vec{k}'}$. A single quantized surface-phonon polariton excitation is written as $|1\rangle_k = \hat{a}_{\vec{k}}^\dagger|0\rangle_k$, with $|0\rangle_k$ the

vacuum state of the system. Furthermore, the field operator for the magnetic field in the upper space is given by

$$\vec{B}_1 = \sqrt{\frac{\hbar\omega}{2\mu_0 S}}\mu_1\mu_0\hat{a}_{\vec{k}}\vec{u}_{1k}e^{ik_p x - i\omega t}e^{-\mathrm{Im}(k_{1z})z} + \mathrm{H.c.} \quad \text{(A60)}$$

This field operator will be used to investigate the magnetic coupling between NV spins and the SPHPs, which allows us to provide a quantum theory to describe the coupling between the NV spin ensemble and the quantized SPHPs.

Note that Ref. [42] studies the classical theory, while here we study the quantum theory of SPHPs. Also, Ref. [42] focuses on bulk modes, while here we focus on surface modes. Other studies focus on piezoelectric superlattices, while here we focus on piezomagnetic ones.

5. Damping of the SPHPs

We consider the SPHP damping associated with the nonradiative loss to the crystal. SPHPs decay nonradiatively due to interacting with the material in the form of phonon scattering, defect scattering, etc, which generally depends on the temperature and the composition of the crystals. The decay of the SPHP mode is frequency dependent, and near the SPHP resonance frequency the SPHP decay is approximately equal to the damping constant of the crystal [20]. If the damping of the material is taken into account, without loss of generality we can add a damping term to the piezomagnetic equations, in which case the permeability function could be written in the form [78,79]

$$\mu_\perp(\omega) = \mu^s_{11}\frac{\omega^2_{\perp o} - \omega^2 - i\kappa\omega}{\omega^2_{\perp L} - \omega^2 - i\kappa\omega}. \quad \text{(A61)}$$

For the surface-phonon polaritons in the presence of damping, a proper damping constant between $\kappa \sim 0.001\omega_{\perp L}$ and $\kappa \sim 0.01\omega_{\perp L}$ can be chosen [78,79]. Another useful figure of merit is the propagation length L_{SPHP}, which can be calculated from the decay time $\tau_{\mathrm{SPHP}} \sim \kappa^{-1}_{\mathrm{SPHP}}$ and group velocity v_g, i.e., $L_{\mathrm{SPHP}} = v_g/\kappa_{\mathrm{SPHP}}$. It is usually larger than the wavelength of SPHP modes in the low dissipation case [43].

APPENDIX B: AN ENSEMBLE OF NV CENTERS INTERACTING WITH THE QUANTIZED MODES OF SPHPS

1. A single NV spin interacting with a single SPHP mode

The interaction of a single NV center located at $\vec{r}_0$ with the total magnetic field can be written as

$$\hat{H}_{\mathrm{NV}} = \hbar D\hat{S}^2_z + \mu_B g_s B_z\hat{S}_z + \mu_B g_s\vec{B}(\vec{r}_0)\cdot\hat{\vec{S}}, \quad \text{(B1)}$$

with $g_s = 2$ the Landé factor of the NV center, μ_B the Bohr magneton, and $\hat{\vec{S}}$ the spin operator of the NV center. In the basis defined by the eigenstates of $\hat{S}_z$, i.e., $\{|m_s\rangle, m_s = 0, \pm 1\}$, with $\hat{S}_z|m_s\rangle = m_s|m_s\rangle$, we get

$$\begin{aligned}\hat{H}_{\mathrm{NV}} &= \sum_{m_s}\{\langle m_s|[\hbar D\hat{S}^2_z + \mu_B g_s B_z\hat{S}_z]|m_s\rangle\}|m_s\rangle\langle m_s| \\ &\quad + \sum_{m_s,m'_s}\{\langle m_s|\mu_B g_s\vec{B}\cdot\hat{\vec{S}}|m'_s\rangle\}|m_s\rangle\langle m'_s| \\ &= \sum_{m_s}\{\hbar D m^2_s + \mu_B g_s B_z m_s\}|m_s\rangle\langle m_s| \\ &\quad + \sum_{m_s,m'_s}\mu_B g_s\hat{B}_x\langle m_s|\hat{S}_x|m'_s\rangle|m_s\rangle\langle m'_s| \\ &\quad + \sum_{m_s}\mu_B g_s m_s\hat{B}_z|m_s\rangle\langle m_s| \\ &= (\hbar D + \mu_B g_s B_z)|+1\rangle\langle+1| + (\hbar D - \mu_B g_s B_z)|-1\rangle \\ &\quad \times\langle -1| + \mu_B g_s B_{z0}(|+1\rangle\langle+1| - |-1\rangle\langle -1|) \\ &\quad \times(\hat{a}^\dagger_{\vec{k}} + \hat{a}_{\vec{k}}) + \frac{\sqrt{2}}{2}\mu_B g_s B_{x0}(\hat{a}_{\vec{k}} + \hat{a}^\dagger_{\vec{k}})(|0\rangle\langle+1| + | \\ &\quad + 1\rangle\langle 0|) + \frac{\sqrt{2}}{2}\mu_B g_s B_{x0}(\hat{a}_{\vec{k}} + \hat{a}^\dagger_{\vec{k}}) \\ &\quad \times(|0\rangle\langle -1| + |-1\rangle\langle 0|). \end{aligned} \quad \text{(B2)}$$

Under the condition $|\Delta/2 + D - \omega(\vec{k})| \ll \Delta/2$, with $\Delta = 2\mu_B g_s B_z/\hbar$, we can neglect the state $|m_s = -1\rangle$, due to the external field moving it far out of resonance. The static magnetic field B_z is about 3 mT that can make the above assumptions valid. This magnetic field is not a strong field, under which the lineal magnetic response of the system still holds. In this case, the static effect of the system is described by the static permeability μ^s_{11} and μ^s_{33}. So the static magnetic field applied to split the NV spin states can be compatible with the piezomagnetic superlattice, and will not affect the SPHP modes. Then under the rotating-wave approximation we can get the following Hamiltonian that describes the interaction between a single NV spin and a SPHP mode $\vec{k}$,

$$\begin{aligned}\hat{\mathcal{H}} &= \frac{1}{2}\hbar\omega_0\hat{\sigma}_z + \hbar\omega(\vec{k})\hat{a}^\dagger_{\vec{k}}\hat{a}_{\vec{k}} \\ &\quad + \frac{\hbar g_\mu(\vec{k}, z_0)}{\sqrt{S}}\hat{\sigma}_+\hat{a}_{\vec{k}}e^{ik_p x_0} + \mathrm{H.c.}\end{aligned} \quad \text{(B3)}$$

2. A NV spin ensemble interacting with the SPHP modes

We now consider the interaction between an ensemble of NV centers and the SPHP modes. As depicted in Fig. 1(a), an ensemble of NV centers is doped into a diamond crystal of thickness h, and located at positions $\vec{r}_i$, each of which with a fixed quantization axis pointing along one of

the four possible crystallographic directions. If the orientations are equally distributed among the four possibilities, and the external field is homogeneous, then a quarter of the NV spins can be made resonant with the SPHP mode. In such a case, we have the following Hamiltonian for N NV spins in the resonant subensemble interacting with the quantized surface mode $\vec{k}$,

$$\hat{\mathcal{H}}_{\vec{k}}^{N} = \sum_{i=1}^{N} \frac{1}{2}\hbar\omega_i \hat{\sigma}_z^i + \hbar\omega(\vec{k})\hat{a}_{\vec{k}}^{\dagger}\hat{a}_{\vec{k}} + \sum_{i=1}^{N} \frac{\hbar g_\mu(\vec{k}, z_i)}{\sqrt{S}}(\hat{\sigma}_+^i \hat{a}_{\vec{k}} e^{ik_p x_i} + \text{H.c.}), \tag{B4}$$

where $\omega_i = \omega_0 + \delta_i \simeq \omega_0$, and δ_i are random offsets accounting for the inhomogeneous broadening of the spin ensemble.

We introduce the collective operators for the spin-wave modes in the NV ensemble

$$\hat{S}_{\vec{k}}^{\dagger} = \frac{1}{\sqrt{N} g_\mu^N(\vec{k})} \sum_{i=1}^{N} g_\mu(\vec{k}, z_i)\hat{\sigma}_+^i e^{ik_p x_i}, \tag{B5}$$

with $g_\mu^N(\vec{k}) = \sqrt{\sum_{i=1}^{N} |g_\mu(\vec{k}, z_i)|^2/N}$. Consider the commutator $[\hat{S}_{\vec{k}}, \hat{S}_{\vec{k}'}^{\dagger}] \equiv D(\vec{k}' - \vec{k})$ in the fully polarized limit:

$$[\hat{S}_{\vec{k}}, \hat{S}_{\vec{k}'}^{\dagger}] = \frac{1}{N}\sum_{i,i'}^{N} \frac{g_\mu(\vec{k}', z_i')g_\mu(\vec{k}, z_i)}{[g_\mu^N(\vec{k})]^2}[\hat{\sigma}_-^i, \hat{\sigma}_+^{i'}]e^{-ik_p x_i}e^{ik_p' x_i'} = \frac{1}{N}\sum_{i}^{N} \frac{g_\mu^2}{(g_\mu^N)^2} e^{i(k_p' - k_p)x_i} \sim \frac{1}{N}\int_{-l/2}^{l/2} e^{i(k_p' - k_p)x} dx, \tag{B6}$$

with l the extent of the sample along the x direction. When $\Delta k = k_p' - k_p = 2\pi/l$, the mode overlap $D(\vec{k}_j - \vec{k}_i) = 0$, which means the spin-wave modes in the strongly polarized limit are orthogonal. We finally get the interaction Hamiltonian for the collective NV spin mode $\hat{S}_{\vec{k}}$ coupled to the SPHP mode $\hat{a}_{\vec{k}}$,

$$\hat{\mathcal{H}}_{\vec{k}}^{I} = \hbar G_\mu^N(\vec{k})\left(\hat{S}_{\vec{k}}^{\dagger}\hat{a}_{\vec{k}} + \text{H.c.}\right). \tag{B7}$$

3. Decoherence of the NV centers

We now consider the decoherence of NV centers in a diamond crystal. In the case of an ensemble of NV centers, there will be magnetic dipole-dipole interactions with other spins like paramagnetic impurities in the diamond crystal, resulting in large dephasing of the NV spins. The coupling of NV spins (S_j) with the surrounding impurity spins (S_k) is [11]

$$H_{\text{spin}} = \hbar \sum_{j,k} S_{j,z}\mathbf{D}_{jk} \cdot \vec{e}_{k,z} S_{k,z}. \tag{B8}$$

The dipole interaction vector is given by

$$\mathbf{D}_{jk} = \frac{\mu_0 g_s^2 \mu_B^2}{4\pi\hbar} \frac{3(\vec{e}_{jk} \cdot \vec{e}_z)\vec{e}_{jk} - \vec{e}_z}{r_{jk}^3}, \tag{B9}$$

with $\vec{e}_z$ the unit vector for the z axis set by the NV crystal axis, r_{jk} the distance between the two spins, and $\vec{e}_{jk}$ a unit vector between them. We can estimate the dephasing for a given spin bath. For a given nitrogen spin density n_N, the typical strength of the spin-spin interaction is about $\mu_0 g_s^2 \mu_B^2 n_N/4\pi\hbar$. This gives the typical dephasing rate of $\gamma_s \sim 2$ MHz for a high nitrogen spin density of $n_N = 10^{19}$ cm^{-3}. Local strain and hyperfine interactions with nearby nuclear spins will also induce dephasing for the NV spins. The typical value of spin dephasing rate for this case is on the order of magnitude less than MHz. Current experiments demonstrate that the dephasing time for a NV spin ensemble is in the microsecond range, with $\gamma_s/2\pi \sim 3$ MHz.

4. The master equation

The full dynamics of our system that takes these incoherent processes into account is described by the master equation [35]

$$\frac{d\hat{\rho}(t)}{dt} = -\frac{i}{\hbar}[\hat{\mathcal{H}}_{\vec{k}}^{I}, \hat{\rho}] + \gamma_s \mathcal{D}[\hat{S}_{\vec{k}}^{\dagger}\hat{S}_{\vec{k}}]\hat{\rho} + \kappa_{\text{SPHP}}\mathcal{D}[\hat{a}_{\vec{k}}]\hat{\rho}, \tag{B10}$$

with $\mathcal{D}[\hat{o}]\hat{\rho} = \hat{o}\hat{\rho}\hat{o}^{\dagger} - \frac{1}{2}\hat{o}^{\dagger}\hat{o}\hat{\rho} - \frac{1}{2}\hat{\rho}\hat{o}^{\dagger}\hat{o}$ for a given operator $\hat{o}$. We assume that the sample is strongly polarized, which can be easily implemented by spin-selective optical pumping, and the number of spin excitations is small compared to N. In the low-excitation limit, the collective spin-wave mode $\hat{S}_{\vec{k}}$ behaves as bosons, i.e., magnons. The lowest two magnon states are the state with all NV spins pointing down, $|0\rangle_{\text{Magn}} = |0_1 0_2 \cdots 0_N\rangle$, and the state with a single magnon excitation $|1_k\rangle_{\text{Magn}} = \hat{S}_{\vec{k}}^{\dagger}|0\rangle_{\text{Magn}}$. Then under the Hamiltonian (9), the system exchanges energy coherently between a quantum of the SPHP mode and a magnon before the decoherence processes dominate the interaction.

5. Eigenfrequencies of the coupled magnon-polariton system

The coupling between the spin-wave mode and the SPHP mode can be determined directly by looking at the eigenfrequencies of the coupled system while the spin ensemble is tuned into resonance with the SPHP mode.

To obtain the system eigenvalues, we consider the non-Hermitian Hamiltonian

$$\hat{H}_{\text{n-H}} = \hbar(\omega_k - i\gamma_s)\hat{S}_{\vec{k}}^{\dagger}\hat{S}_{\vec{k}} + \hbar[\omega(\vec{k}) - i\kappa_{\text{SPHP}}]\hat{a}_{\vec{k}}^{\dagger}\hat{a}_{\vec{k}} + \hbar G_{\mu}^{N}(\vec{k})(\hat{S}_{\vec{k}}^{\dagger}\hat{a}_{\vec{k}} + \text{H.c.}). \tag{B11}$$

Using the non-Hermitian Hamiltonian where the decays are taken into account, the eigenenergies and the broadenings of the coupled system can be obtained as the real and imaginary parts of the eigenvalues, respectively. The eigenvalues of $\hat{H}_{\text{n-H}}$ are given by

$$E^{\pm} = \hbar\left(\frac{\omega_k + \omega(\vec{k}) - i(\gamma_s + \kappa_{\text{SPHP}})}{2} \pm \left\{(G_{\mu}^{N})^2 + \frac{1}{4}[\omega_k - \omega(\vec{k}) - i(\gamma_s + \kappa_{\text{SPHP}})]^2\right\}^{1/2}\right). \tag{B12}$$

Then we obtain the eigenfrequencies of the coupled magnon-polariton system $\omega_{\pm} = \text{Re}(E^{\pm})/\hbar$.

[1] L. Childress, M. V. Gurudev Dutt, J. M. Taylor, A. S. Zibrov, F. Jelezko, J. Wrachtrup, P. R. Hemmer, and M. D. Lukin, Coherent dynamics of coupled electron and nuclear spin qubits in diamond, Science **314**, 281 (2006).

[2] M. Steger, K. Saeedi, M. L. W. Thewalt, J. J. L. Morton, H. Riemann, N. V. Abrosimov, P. Becker, and H.-J. Pohl, Quantum information storage for over 180 s using donor spins in a $^{2}8$Si "semiconductor vacuum", Science **336**, 1280 (2012).

[3] Ronald Hanson and David D. Awschalom, Coherent manipulation of single spins in semiconductors, Nature (London) **453**, 1043 (2008).

[4] T. Gaebel, M. Domhan, I. Popa, C. Wittmann, P. Neumann, F. Jelezko, J. R. Rabeau, N. Stavrias, A. D. Greentree, S. Prawer, J. Meijer, J. Twamley, P. R. Hemmer, and J. Wrachtrup, Room-temperature coherent coupling of single spins in diamond, Nat. Phys. **2**, 408 (2010).

[5] A. Tyryshkin, S. Tojo, J. Morton, H. Riemann, N. Abrosimov, P. Becker, H.-J. Pohl, T. Schenkel, M. Thewalt, K. Itoh, and S. Lyon, Electron spin coherence exceeding seconds in high-purity silicon, Nat. Mater. **11**, 143 (2012).

[6] N. Bar-Gill, L. M. Pham, A. Jarmola, D. Budker, and R. L. Walsworth, Solid-state electronic spin coherence time approaching one second, Nat. Commun. **4**, 1743 (2013).

[7] D. I. Schuster, A. P. Sears, E. Ginossar, L. DiCarlo, L. Frunzio, J. J. L. Morton, H. Wu, G. A. D. Briggs, B. B. Buckley, D. D. Awschalom, and R. J. Schoelkopf, High-cooperativity Coupling of Electron-spin Ensembles to Superconducting Cavities, Phys. Rev. Lett. **105**, 140501 (2010).

[8] M. W. Doherty, N. B. Manson, P. Delaney, F. Jelezko, J. Wrachtrup, and Lloyd C. L. Hollenberg, The nitrogen-vacancy colour centre in diamond, Phys. Rep. **528**, 1 (2013).

[9] B. C. Rose, A. M. Tyryshkin, H. Riemann, N. V. Abrosimov, P. Becker, H.-J. Pohl, M. L. W. Thewalt, K. M. Itoh, and S. A. Lyon, Coherent Rabi Dynamics of a Superradiant Spin Ensemble in a Microwave Cavity, Phys. Rev. X **7**, 031002 (2017).

[10] Y. Kubo, F. R. Ong, P. Bertet, D. Vion, V. Jacques, D. Zheng, A. Dreau, J.-F. Roch, A. Auffeves, F. Jelezko, J. Wrachtrup, M. F. Barthe, P. Bergonzo, and D. Esteve, Strong Coupling of a Spin Ensemble to a Superconducting Resonator, Phys. Rev. Lett. **105**, 140502 (2010).

[11] D. Marcos, M. Wubs, J. M. Taylor, R. Aguado, M. D. Lukin, and A. S. Srensen, Coupling Nitrogen-vacancy Centers in Diamond to Superconducting Flux Qubits, Phys. Rev. Lett. **105**, 210501 (2010).

[12] R. Amsuss, Ch. Koller, T. Nobauer, S. Putz, S. Rotter, K. Sandner, S. Schneider, M. Schrambock, G. Steinhauser, H. Ritsch, J. Schmiedmayer, and J. Majer, Cavity QED with Magnetically Coupled Collective Spin States, Phys. Rev. Lett. **107**, 060502 (2011).

[13] S. Putz, D. O. Krimer, R. Amsüss, A. Valookaran, T. Nöbauer, J. Schmiedmayer, S. Rotter, and J. Majer, Protecting a spin ensemble against decoherence in the strong-coupling regime of cavity QED, Nat. Phys. **10**, 720 (2014).

[14] Xiaobo Zhu, Shiro Saito, Alexander Kemp, Kosuke Kakuyanagi, Shin ichi Karimoto, Hayato Nakano, William J. Munro, Yasuhiro Tokura, Mark S. Everitt, Kae Nemoto, Makoto Kasu, Norikazu Mizuochi, and Kouichi Semba, Coherent coupling of a superconducting flux qubit to an electron spin ensemble in diamond, Nature **478**, 221 (2011).

[15] J. H. Wesenberg, A. Ardavan, G. A. D. Briggs, J. J. L. Morton, R. J. Schoelkopf, D. I. Schuster, and K. Mlmer, Quantum Computing with an Electron Spin Ensemble, Phys. Rev. Lett. **103**, 070502 (2009).

[16] Hua Wu, Richard E. George, Janus H. Wesenberg, Klaus Mlmer, David I. Schuster, Robert J. Schoelkopf, Kohei M. Itoh, Arzhang Ardavan, John J. L. Morton, and G. Andrew D. Briggs, Storage of Multiple Coherent Microwave Excitations in an Electron Spin Ensemble, Phys. Rev. Lett. **105**, 140503 (2010).

[17] C. Grezes, B. Julsgaard, Y. Kubo, M. Stern, T. Umeda, J. Isoya, H. Sumiya, H. Abe, S. Onoda, T. Ohshima, V. Jacques, J. Esteve, D. Vion, D. Esteve, K. Mlmer, and P. Bertet, Multimode Storage and Retrieval of Microwave Fields in a Spin Ensemble, Phys. Rev. X **4**, 021049 (2014).

[18] Karl Tordrup, Antonio Negretti, and Klaus Mlmer, Holographic Quantum Computing, Phys. Rev. Lett. **101**, 040501 (2008).

[19] A. Hartstein, E. Burstein, A. A. Maradudin, R. Brewer, and R. F. Wallis, Surface polaritons on semi-infinite gyromagnetic media, J. Phys. C: Solid State Phys. **6**, 1266 (1973).

[20] J. Nkoma, R. Loudon, and D. R. Tilley, Elementary properties of surface polaritons, J. Phys. C: Solid State Phys. **7**, 3547 (1974).

[21] E. Burstein, W. P. Chen, Y. J. Chen, and A. Hartstein, Surface polaritons—propagating electromagnetic modes at interfaces, J. Vac. Sci. Technol. **11**, 1004 (1974).
[22] G. Borstel and H. J. Falge, Surface polaritons in semi-infinite crystals, Appl. Phys. **16**, 211 (1978).
[23] D. L. Mills and E. Burstein, Polaritons: The electromagnetic modes of media, Rep. Prog. Phys. **37**, 817 (1974).
[24] J. M. Pitarke, V. M. Silkin, E. V. Chulkov, and P. M. Echenique, Theory of surface plasmons and surface-plasmon polaritons, Rep. Prog. Phys. **70**, 1 (2006).
[25] William L. Barnes, Alain Dereux, and Thomas W. Ebbesen, Surface plasmon subwavelength optics, Nature **424**, 824 (2003).
[26] D. E. Chang, A. S. Srensen, P. R. Hemmer, and M. D. Lukin, Quantum Optics with Surface Plasmons, Phys. Rev. Lett. **97**, 053002 (2006).
[27] M. S. Tame, C. Lee, J. Lee, D. Ballester, M. Paternostro, A. V. Zayats, and M. S. Kim, Single-photon Excitation of Surface Plasmon Polaritons, Phys. Rev. Lett. **101**, 190504 (2008).
[28] A. V. Akimov, A. Mukherjee, C. L. Yu, D. E. Chang, A. S. Zibrov, P. R. Hemmer, H. Park, and M. D. Lukin, Generation of single optical plasmons in metallicnanowires coupled to quantum dots, Nature **450**, 402 (2007).
[29] J. Bellessa, C. Bonnand, J. C. Plenet, and J. Mugnier, Strong Coupling between Surface Plasmons and Excitons in an Organic Semiconductor, Phys. Rev. Lett. **93**, 036404 (2004).
[30] T. K. Hakala, J. J. Toppari, Anton Kuzyk, M. Pettersson, H. Tikkanen, H. Kunttu, and Päivi Törmä, Vacuum Rabi Splitting Andstrong-coupling Dynamics for Surface-plasmon Polaritons and Rhodamine6G Molecules, Phys. Rev. Lett. **103**, 053602 (2009).
[31] Alexander Huck, Shailesh Kumar, Abdul Shakoor, and Ulrik L. Andersen, Controlled Coupling of a Single Nitrogen-vacancy Center to a Silver Nanowire, Phys. Rev. Lett. **106**, 096801 (2011).
[32] S. Aberra Guebrou, C. Symonds, E. Homeyer, J. C. Plenet, Yu. N. Gartstein, V. M. Agranovich, and J. Bellessa, Coherent Emission from a Disordered Organic Semiconductor Induced by Strong Coupling with Surface Plasmons, Phys. Rev. Lett. **108**, 066401 (2012).
[33] P. Törmä and William L. Barnes, Strong coupling between surface plasmon polaritons and emitters: A review, Rep. Prog. Phys. **78**, 013901 (2014).
[34] Harald Kübler, J. P. Shaffer, T. Baluktsian, R. Löw, and T. Pfau, Coherent excitation of Rydbergatoms in micrometre-sized atomic vapour cells, Nat. Photon. **4**, 112 (2010).
[35] A. González-Tudela, P. A. Huidobro, L. Martń-Moreno, C. Tejedor, and F. J. Garcá-Vidal, Theory of Strong Coupling between Quantum Emitters and Propagating Surface Plasmons, Phys. Rev. Lett. **110**, 126801 (2013).
[36] S. Dai, Z. Fei, Q. Ma, A. S. Rodin, M. Wagner, A. S. McLeod, M. K. Liu, W. Gannett, W. Regan, K. Watanabe, T. Taniguchi, M. Thiemens, G. Dominguez, A. H. Castro Neto, A. Zettl, F. Keilmann, P. Jarillo-Herrero, M. M. Fogler, and D. N. Basov, Tunable phonon polaritons in atomically thin van der Waals crystals of boron nitride, Science **343**, 1125 (2014).
[37] Joshua D. Caldwell, Andrey V. Kretinin, Yiguo Chen, Vincenzo Giannini, Michael M. Fogler, Yan Francescato, Chase T. Ellis, Joseph G. Tischler, Colin R. Woods, Alexander J. Giles, Minghui Hong, Kenji Watanabe, Takashi Taniguchi, Stefan A. Maier, and Kostya S. Novoselov, Sub-diffractional volume-confined polaritons in the natural hyperbolic material hexagonal boron nitride, Nat. Commun. **5**, 5221 (2014).
[38] Xiaoji G. Xu, Behnood G. Ghamsari, Jian-Hua Jiang, Leonid Gilburd, Gregory O. Andreev, Chunyi Zhi, Yoshio Bando, Dmitri Golberg, Pierre Berini, and Gilbert C. Walker, One-dimensional surface phonon polaritons in boron nitride nanotubes, Nat. Commun. **5**, 4782 (2014).
[39] Yan-qing Lu, Yong-yuan Zhu, Yan-feng Chen, Shi-ning Zhu, Nai-ben Ming, and Yi-Jun Feng, Optical properties of an ionic-type phononic crystal, Science **284**, 1822 (1999).
[40] Yong-yuan Zhu, Xue-jin Zhang, Yan-qing Lu, Yan-feng Chen, Shi-ning Zhu, and Nai-ben Ming, New Type of Polariton in a Piezoelectric Superlattice, Phys. Rev. Lett. **90**, 053903 (2003).
[41] Ruo-Cheng Yin, Cheng He, Ming-Hui Lu, Yan-Qing Lu, and Yan-Feng Chen, Polaritons in an artificial ionic-type crystal made of two-dimensional periodically inversed multi-domain ferroelectric crystals, J. Appl. Phys. **109**, 064110 (2011).
[42] H. Liu, S. N. Zhu, Z. G. Dong, Y. Y. Zhu, Y. F. Chen, N. B. Ming, and Xiang Zhang, Coupling of electromagnetic waves and superlattice vibrations in a piezomagnetic superlattice: Creation of a polariton through the piezomagnetic effect, Phys. Rev. B **71**, 125106 (2005).
[43] Xi-kui Hu, Yang Ming, Xue-jin Zhang, Yan-qing Lu, and Yong-yuan Zhu, Mimicing surface phonon polaritons in microwave band based on ionic-type phononic crystal, Appl. Phys. Lett. **101**, 151109 (2012).
[44] Jiteng Sheng, Yuanxi Chao, and James P. Shaffer, Strong Coupling of Rydberg Atoms and Surface Phonon Polaritons on Piezoelectric Superlattices, Phys. Rev. Lett. **117**, 103201 (2016).
[45] Ze-Liang Xiang, Sahel Ashhab, J. Q. You, and Franco Nori, Hybrid quantum circuits: Superconducting circuits interacting with other quantum systems, Rev. Mod. Phys. **85**, 623 (2013).
[46] J. Verdú, H. Zoubi, Ch. Koller, J. Majer, H. Ritsch, and J. Schmiedmayer, Strong Magnetic Coupling of an Ultracold Gas to a Superconducting Waveguide Cavity, Phys. Rev. Lett. **103**, 043603 (2009).
[47] Peng-Bo Li, Ze-Liang Xiang, Peter Rabl, and Franco Nori, Hybrid Quantum Device with Nitrogen-vacancy Centers in Diamond Coupled to Carbon Nanotubes, Phys. Rev. Lett. **117**, 015502 (2016).
[48] Peng-Bo Li, Yong-Chun Liu, S.-Y. Gao, Ze-Liang Xiang, Peter Rabl, Yun-Feng Xiao, and Fu-Li Li, Hybrid Quantum Device based on NV Centers in Diamond Nanomechanical Resonators Plus Superconducting Waveguide Cavities, Phys. Rev. Applied **4**, 044003 (2015).
[49] A. André, D. DeMille, J. M. Doyle, M. D. Lukin, S. E. Maxwell, P. Rabl, R. J. Schoelkopf, and P. Zoller, A

coherent all-electrical interface between polar molecules and mesoscopic superconducting resonators, Nat. Phys. **2**, 636 (2006).

[50] P. Rabl, D. DeMille, J. M. Doyle, M. D. Lukin, R. J. Schoelkopf, and P. Zoller, Hybrid Quantum Processors: Molecular Ensembles as Quantum Memory for Solid State Circuits, Phys. Rev. Lett. **97**, 033003 (2006).

[51] Atac Imamoğlu, Cavity QED based on Collective Magnetic Dipole Coupling: Spin Ensembles as Hybrid Two-level Systems, Phys. Rev. Lett. **102**, 083602 (2009).

[52] Xin-You Lv, Ze-Liang Xiang, Wei Cui, J. Q. You, and Franco Nori, Quantum memory using a hybrid circuit with flux qubits and nitrogen-vacancy centers, Phys. Rev. A **88**, 012329 (2013).

[53] Ze-Liang Xiang, Xin-You Lv, Tie-Fu Li, J. Q. You, and Franco Nori, Hybrid quantum circuit consisting of a superconducting flux qubit coupled to a spin ensemble and a transmission-line resonator, Phys. Rev. B **87**, 144516 (2013).

[54] Paolo Andrich, Charles F. de las Casas, Xiaoying Liu, Hope L. Bretscher, Jonson R. Berman, F. Joseph Heremans, Paul F. Nealey, and David D. Awschalom, Long-range spin wave mediated control of defect qubits in nanodiamonds, npj Quantum Information **3**, 28 (2017).

[55] Joshua D. Caldwell, Lucas Lindsay, Vincenzo Giannini, Igor Vurgaftman, Thomas L. Reinecke, Stefan A. Maier, and Orest J. Glembocki, Low-loss, infrared and terahertz nanophotonics using surface phonon polaritons, Nanophotonics **4**, 44 (2015).

[56] Inigo Liberal and Nader Engheta, Near-zero refractive index photonics, Nat. Photon. **11**, 149 (2017).

[57] Joshua D. Caldwell, Orest J. Glembocki, Yan Francescato, Nicholas Sharac, Vincenzo Giannini, Francisco J. Bezares, James P. Long, Jeffrey C. Owrutsky, Igor Vurgaftman, Joseph G. Tischler, Virginia D. Wheeler, Nabil D. Bassim, Loretta M. Shirey, Richard Kasica, and Stefan A. Maier, Low-loss, extreme subdiffraction photon confinement via silicon carbide localized surface phonon polariton resonators, Nano Lett. **13**, 3690 (2013).

[58] Yiguo Chen, Yan Francescato, Joshua D. Caldwell, Vincenzo Giannini, Tobias W. W. Maß, Orest J. Glembocki, Francisco J. Bezares, Thomas Taubner, Richard Kasica, Minghui Hong, and Stefan A. Maier, Spectral tuning of localized surface phonon polariton resonators for low-loss mid-IR applications, ACS Photonics **1**, 718–724 (2014).

[59] A. González-Tudela, C.-L. Hung, D. E. Chang, J. I. Cirac, and H. J. Kimble, Subwavelength vacuum lattices and atom-atom interactions in two-dimensional photonic crystals, Nat. Photon. **9**, 320 (2015).

[60] Zubin Jacob and Vladimir M. Shalaev, Plasmonics goes quantum, Science **334**, 463 (2011).

[61] M. S. Tame, S. K. Ozdemir, S. A. Maier, J. Lee, K. R. McEnery, and M. S. Kim, Quantum plasmonics, Nat. Phys. **9**, 329 (2010).

[62] Sergey I. Bozhevolnyi and Jacob B. Khurgin, The case for quantum plasmonics, Nat. Photon. **11**, 398 (2017).

[63] Pavel Ginzburg, Cavity quantum electrodynamics in application to plasmonics and metamaterials, Rev. Phys. **1**, 120 (2016).

[64] See Appendices for more details.

[65] Edward Yoxall, Martin Schnell, Alexey Y. Nikitin, Oihana Txoperena, Achim Woessner, Mark B. Lundeberg, Félix Casanova, Luis E. Hueso, Frank H. L. Koppens, and Rainer Hillenbrand, Direct observation of ultraslow hyperbolic polariton propagation with negative phase velocity, Nat. Photon. **9**, 674 (2015).

[66] K. Y. Bliokh, A. Y. Bekshaev, and F. Nori, Extraordinary momentum and spin in evanescent waves, Nat. Commun. **5**, 3300 (2014).

[67] K. Y. Bliokh, D. Smirnova, and F. Nori, Quantum spin Hall effect of light, Science **348**, 1448 (2015).

[68] Jiangfeng Du, Xing Rong, Nan Zhao, Ya Wang, Jiahui Yang, and R. B. Liu, Preserving electron spin coherence in solids by optimal dynamical decoupling, Nature **461**, 1265 (2009).

[69] A. J. Huber, B. Deutsch, L. Novotny, and R. Hillenbrand, Focusing of surface phonon polaritons, Appl. Phys. Lett. **92**, 203104 (2008).

[70] A. Angerer, K. Streltsov, T. Astner, S. Putz, H. Sumiya, S. Onoda, J. Isoya, W. J. Munro, K. Nemoto, J. Schmiedmayer, and J. Majer, Superradiant hybrid quantum devices, arXiv:1802.07100v1[quant-ph].

[71] Jin-xi Liu, Dai-Ning Fang, Wei-Yi Wei, and Xiao-Fang Zhao, Love waves in layered piezoelectric/piezomagnetic structures, J. Sound Vib. **315**, 146 (2008).

[72] Fernando Ramireza, Paul R. Heyligera, and Ernian Pan, Free vibration response of two-dimensional magneto-electro-elastic laminated plates, J. Sound Vib. **292**, 626 (2006).

[73] R. Warmbier, G. S. Manyali, and A. Quandt, Surface plasmon polaritons in lossy uniaxial anisotropic materials, Phys. Rev. B **85**, 085442 (2012).

[74] A. E. Giannakopoulos and A. Z. Parmaklis, The contact problem of a circular rigid punch on piezomagnetic materials, Int. J. Solids Struct. **44**, 4593 (2007).

[75] Y. P. Yao, Y. Hou, S. N. Dong, and X. G. Li, Giant magnetodielectric effect in Terfenol-D/PZT magnetoelectric laminate composite, J. Appl. Phys. **110**, 014508 (2011).

[76] L. D. Landau and E. M. Lifshitz, *Electrodynamics of Continuous Media* (Pergamon Press, Oxford, 1984).

[77] A. Archambault, F. Marquier, J.-J. Greffet, and C. Arnold, Quantum theory of spontaneous and stimulated emission of surface plasmons, Phys. Rev. B **82**, 035411 (2010).

[78] X. J. Zhang, R. Q. Zhu, J. Zhao, Y. F. Chen, and Y. Y. Zhu, Phonon-polariton dispersion and the polariton-based photonic band gap in piezoelectric superlattices, Phys. Rev. B **69**, 085118 (2004).

[79] Jun Zhao, Ruo-Cheng Yin, Tian Fan, Ming-Hui Lu, Yan-Feng Chen, Yong-Yuan Zhu, Shi-Ning Zhu, and Nai-Ben Ming, Coupled phonon polaritons in a piezoelectric-piezomagnetic superlattice, Phys. Rev. B **77**, 075126 (2008).